PROCEEDINGS OF SPIE

SPIEDigitalLibrary.org/conference-proceedings-of-spie

Optic disc segmentation in fundus images using deep learning

Jongwoo Kim, Loc Tran, Emily Y. Chew, Sameer Antani, George R. Thoma

Jongwoo Kim, Loc Tran, Emily Y. Chew, Sameer Antani, George R. Thoma, "Optic disc segmentation in fundus images using deep learning," Proc. SPIE 10954, Medical Imaging 2019: Imaging Informatics for Healthcare, Research, and Applications, 109540H (15 March 2019); doi: 10.1117/12.2512798

SPIE.

Event: SPIE Medical Imaging, 2019, San Diego, California, United States

Optic Disc Segmentation in Fundus Images Using Deep Learning

Jongwoo Kim *[a], Loc Tran[a], Emily Y. Chew[b], Sameer Antani[a], and George R. Thoma[a]
[a] Lister Hill National Center for Biomedical Communications, National Library of Medicine, Bethesda, MD, USA; [b] Division of Epidemiology & Clinical Applications, National Eye Institute, National Institutes of Health, Bethesda, MD, USA

ABSTRACT

Ophthalmologists use the optic disc to cup ratio as one factor to diagnose glaucoma. Optic disc in fundus images is the area where blood vessels and optic nerve fibers enter the retina. A cup to disc ratio (the diameter of the cup divided by the diameter of the optic disc) greater than 0.3 is considered to be suggestive of glaucoma. Therefore, we are developing automatic methods to estimate optic disc and cup areas, and the optic disc to cup ratio. There are four steps to estimate the ratio: region of interest (ROI) area detection (where optic disc is in the center) from the fundus image, optic disc segmentation from the ROI, cup segmentation from the optic disc area, and cup to optic disc ratio estimation. This paper proposes an automated method to segment the optic disc from the ROI using deep learning. A Fully Convolutional Network (FCN) with a U-Net architecture is used for the segmentation. We use fundus images from MESSIDOR dataset in this experiment, a public dataset containing 1,200 fundus images. We divide the dataset into five equal subsets for training and independent testing (each set has four subsets for training and one subset for testing). The proposed method outperforms other existing algorithms. The results show 0.94 Jaccard index, 0.98 sensitivity, 0.99 specificity, and 0.99 accuracy.

Keywords: Glaucoma, Region of Interest (ROI), Optic Disc, Deep Learning, Fully Convolutional Networks (FCN), U-Net

1. INTRODUCTION

Glaucoma is a complex eye disease that damages the optic nerve, resulting in irreversible vision loss. It is diagnosed with visual field defects, optic nerve abnormalities with enlarged cup to optic disc ratios and often elevated intraocular pressures. However, in some cases, intraocular pressures may not be elevated (low tension glaucoma). Patients may be asymptomatic until significant vision is lost since there are no early warning symptoms. The potential mechanisms for increased intraocular pressure are currently undergoing evaluation. In most types of glaucoma, high intraocular pressure damages/kills the optic nerve and this makes the cup become larger in comparison to the optic disc.-A cup to disc ratio (the diameter of the cup divided by the diameter of the optic disc) greater than 0.3 is considered to be suspicious for glaucoma [1]. Unfortunately, high subjectivity has been noted among ophthalmologists in segmenting the optic disc and cup areas. I.e., ophthalmologists cannot grade the ratio consistently [2]. Therefore, we are developing an algorithm to segment the areas using a Fully Convolutional Network (FCN) and to estimate the ratio automatically. Optic disc and cup detection is also important to diagnose other eye diseases since we can distinguish optic disc/cup from large exudative lesions in fundus images using the algorithm. Optic disc segmentation in fundus images is a challenging problem due to the variation of optic disc such as size, shape, color, etc. There are several methods used to process fundus images to segment the optic disc and cup. First, estimate blood vessels using different thresholding methods since blood vessels are emanating from the cup [2, 3, 4, 5, 6, 7]. Second, estimate bright regions for optic disc candidate regions using thresholding methods [2] and estimate the probability of probable optic disc in each region using blood vessels and features extracted from the candidate regions [4, 6]. Third, use ellipse fitting methods to estimate the final optic disc area [4, 6, 7]. A geometrical method is also used based on blood vessel information since blood vessels are emanating from the optic disc and their paths follow a similar directional patterns [5]. In most cases, the performance of the algorithms depends on binarization algorithms for estimating candidate optic discs with the assumption that optic discs have the brightest pixel values. In addition, it also depends on good binary blood vessel detection algorithms since they heavily depend on blood vessel information. Therefore, a good binarization algorithm is key for the performance of the methods. Machine learning algorithms such as support vector machine (SVM) have also been used recently for segmentation [8, 9]. Ellipse fitting is necessary as the last step to find missing optic disc areas due to blood vessels or incorrect optic disc segmentation results [3, 6, 7, 8]. Deep learning is recently adapted to improve images [10] and segment blood vessels [10, 11]. Convolutional Neural Networks (CNN) is also adapted in optic disc and cup boundary segmentation [12]. However, it needs preprocessing to remove blood vessels and post processing to segment the boundaries from probability matrices estimated by the CNN [12]. The method needs a long computation time to estimate probability of each pixel.

*jongkim@mail.nih.gov; phone 1 301 435-3227; fax 1 301 402-0341; https://www.nlm.nih.gov

Medical Imaging 2019: Imaging Informatics for Healthcare, Research, and Applications,
edited by Po-Hao Chen, Peter R. Bak, Proc. of SPIE Vol. 10954, 109540H

Updated 3/20/14

Therefore, we propose a new method to segment the optic disc without preprocessing using a FCN. The FCN uses a whole image as an input and outputs a segmentation result as a final result. There is no post processing for fine tuning (such as a boundary smoothing process) to finalize optic disc area. In the following sections of the paper, we introduce our dataset. Then we describe our method, followed by our experimental results. Finally, we describe our future research work.

2. DATASETS

We use publicly available fundus image dataset called MESSIDOR [13] which has 1,200 fundus images. Among them, 800 images are acquired by pupil dilation and 400 are without dilation. The image sizes are either 1,440×960, 2,240×1,488, or 2,304×1,536. This dataset contains other data such as diabetic retinopathy grade, risk of edema, and optic disc for each image.

3. METHOD

There are four steps to estimate the ratio in our method. First, region of interest detection (ROI) from fundus images is established where the optic disc is in the center. Second, optic disc segmentation is performed from the ROI. Third, cup segmentation from the optic disc is conducted. Fourth, the optic disc to cup ratio is estimated. We will focus on the method to segment the optic disc from the ROI using deep learning algorithm (CNNs) in this paper.

3.1 ROI detection

A CNN is used to detect ROI areas [3]. The structure of the CNN is composed of two convolutional layers, two max pooling layers, two fully connected layers, and one output layer. We first crop images for ROI and Non-ROI image classes from the training fundus image set and train the CNN using the image classes. The following steps are then used to find the ROI from fundus images. First, binarize an input fundus image to estimate retina using Otsu threshold and estimate an ellipse that fits to the edge of the retina. Second, set the window size W = longest diameter of the ellipse/3.5 and stride S = W/4. Third, Move $W \times W$ window to the horizontal and vertical directions by S, estimate a CNN result of each window, and choose a window W_1 that has the highest result as the ROI of the image. Figure 1 shows ROI estimation Results. Green boxes in the images show the ROI estimated by [3].

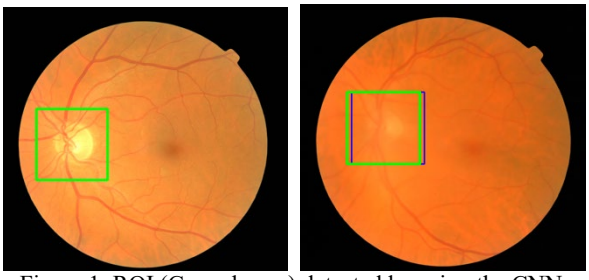

Figure 1. ROI (Green boxes) detected by using the CNN.

3.2 Optic disc segmentation from ROI

A FCN model called U-Net [14] is used extensively in biomedical image segmentation. Therefore, we implement a U-Net using Tensorflow with Keras to segment the optic disc from the ROI in fundus images. Figure 2 shows the architecture of the FCN that we use. Input of the proposed FCN is 224×224×3 color images and output is 224×224×1 labeled binary images. We add two dropout layers to train the FCN more robustly. The FCN has two paths. The contracting path (left side) has the typical FCN architecture consisting of convolutional layers and max pooling layers. The expansive path (right side) consists of an upsampling of the feature map followed by convolutional layers. The final convolutional layer maps each feature vector to the desired number of classes. In the case of conventional CNNs, output of the CNNs is class labels. Therefore, the CNNs need to run $N \times N$ times to segment an $N \times N$ input image [12]. However, the FCN assigns a class label to each pixel as an output. Therefore, FCN needs much less computation time.

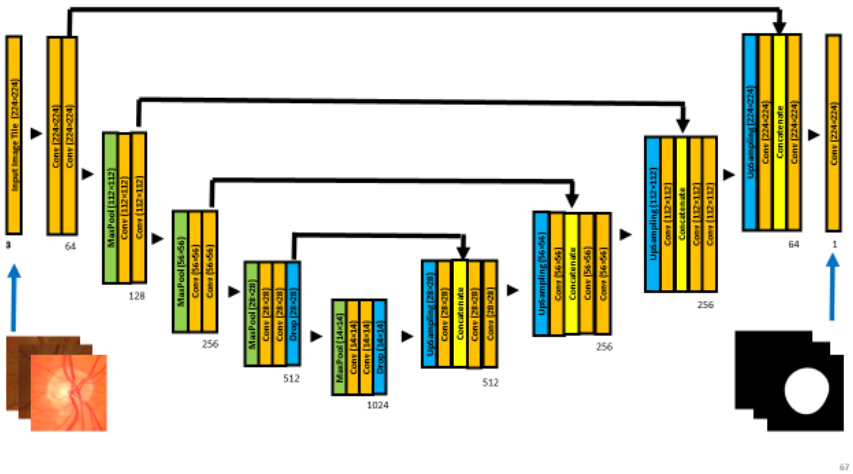

Figure. 2. FCN architecture (U-Net) used in this experiment.

4. EXPERIMENTAL RESULTS AND DISCUSSION

In this section, we present the experimental test results for the second step in detail. From the MESSIDOR dataset, we collect 1,200 train and test images by cropping the ROIs manually. The cropped image sizes are 400×400 or 250×250 depending on fundus image sizes. We then normalize the images to 224×224 for training the FCN. There are not many images for training and testing for the FCN. Therefore, we divide the dataset into five equal subsets to make five different sets for training and testing (each set has four subsets for training and one subset for testing). We then train and test the five different sets independently. Each set contains 960 training images and 240 test images. We use a maximum of 200 epochs, learning rate = 0.0001, Adam optimization algorithm for training, and save the best results as output of the training results during the training time. We use NVIDIA GeForce GTX1080-Ti for training and average training time is 2 hours 17 minutes. Figure 3 shows some test results. The first column shows input ROI images, the second column shows ground truth optic disc images, and the third column shows optic disc images from the proposed FCN. The last column shows optic disc boundaries of ground truth and our estimation results. Green color represents ground truth optic disc and blue color means our results. Figure 4 shows more test results. Estimated boundaries (blue color) are very close to ground truth (green color) boundaries. In case of the image in the second row third column, our result is more accurate than the ground truth result. Figure 5 shows the diagram used to evaluate the performance. We define ground truth optic disc (green color) as G and estimated optic disc (blue color) as E. $G \cap E$ area means the FCN correctly segments optic disc area (TP), FN means the FCN missed ground truth area, and FP means the FCN mislabeled non-ground truth area as optic disc area. TN means the FCN correctly classifies non-optic disc area. We evaluate the performance of the FCN using Jaccard index, sensitivity, specificity, and accuracy as shown in the equations (1) to (4). Table 1 shows the training and test results for each set. The third set shows the best performance on Jaccard index and accuracy, the fourth set shows the best performance on specificity, and the fifth set shows the best performance on sensitivity. The FCN shows 0.9386 Jaccard index, 0.9680 sensitivity, 0.9914 specificity, and 0.9857 accuracy in average. Table 2 shows performance measures as function of the Measure Ratio R. The first row means 61.67% of test images have over 0.95 Jaccard index, 88.33% have over 0.95 sensitivity, 99.17% have over 0.95 specificity, and 100% have over 0.95 accuracy. Specificity and accuracy use TN as a parameter and number of TN becomes smaller if the optic discs are estimated from the ROIs (our case) instead of whole fundus images. Some algorithms estimate optic discs from whole fundus images and some are from the ROIs. It is hard to compare the performance of the algorithms using the two measures since they have different numbers of TN. Therefore, we use Jaccard index and sensitivity that do not use TN to compare the performance of the proposed FCN with other algorithms using MESSIDOR dataset. Table 3 shows comparison of our results with others. The proposed FCN shows better results than other algorithms. In the case of Jaccard index, the best ratio of other methods is 0.87 while the proposed FCN shows 0.94. In the case of sensitivity, the best ratio of other method is 0.93 while the proposed FCN shows 0.97.

$$Jaccard\ Index = \frac{G \cap E}{G \cup E} \quad (1)$$

$$Sensitivity\ (SEN) = \frac{TP}{TP+FN} \quad (2)$$

$$Specificity\ (SPE) = \frac{TN}{TN+FP} \quad (3)$$

$$Accuracy\ (ACC) = \frac{TP+TN}{TP+TN+FP+FN} \quad (4)$$

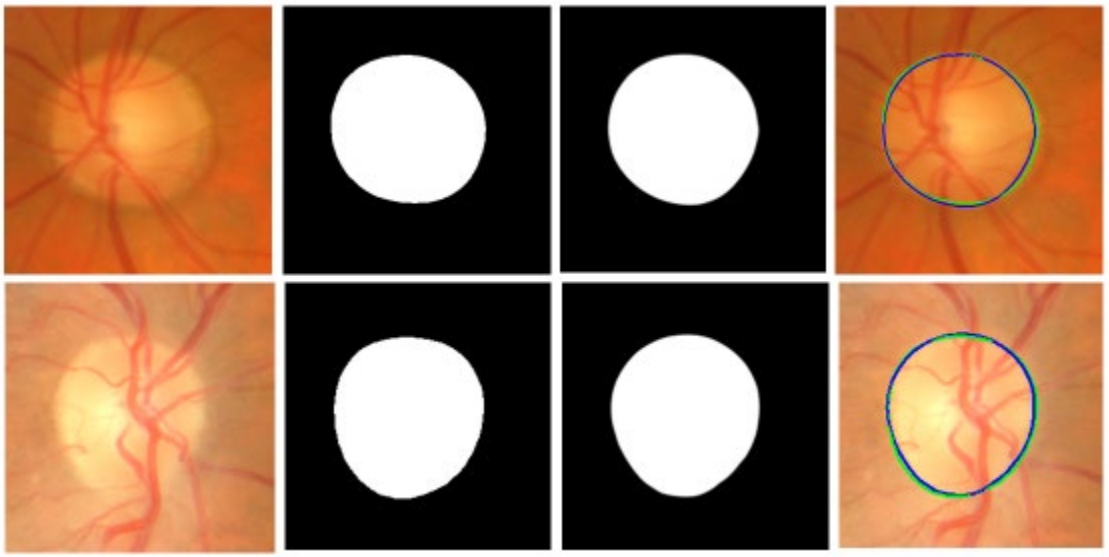

(a) (b) (c) (d)

Figure 3. Optic disc segmentation results using the proposed FCN. Green color is ground truth and blue color is estimated results. (a) Input ROI images, (b) Ground truth results, (c) Estimated results, and (d) Overlapped results.

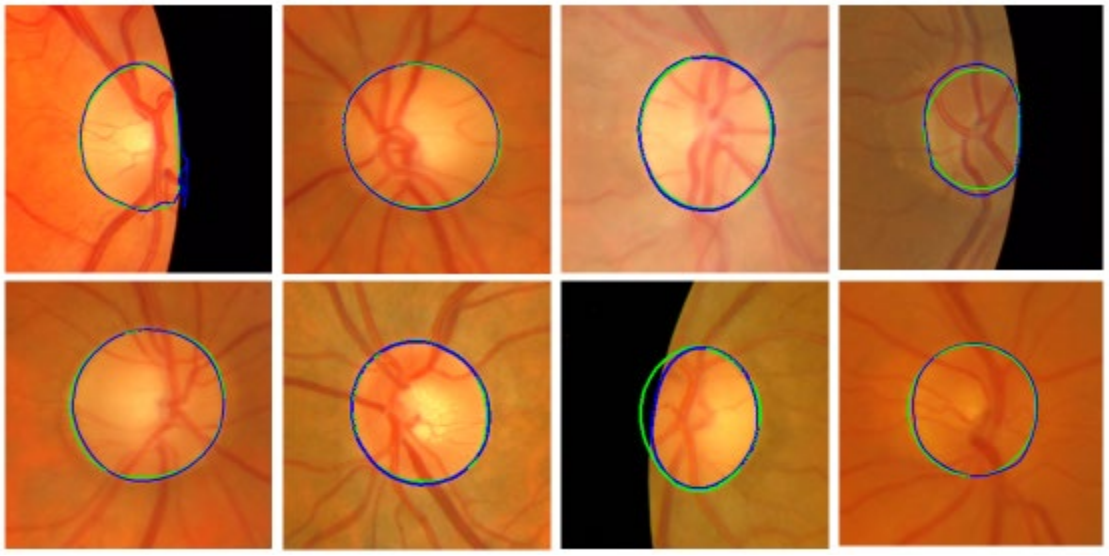

Figure 4. Optic disc segmentation results using the proposed FCN. Green color is ground truth and blue color is estimated results.

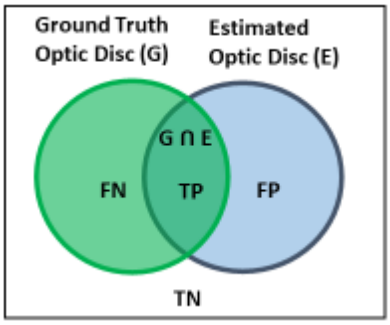

Figure 5. Diagram used to evaluation the performance

Table 1. Evaluation results of each dataset using the four different measure.

Set	Jaccard Index	Sensitivity	Specificity	Accuracy
1	0.9312	0.9649	0.9905	0.9845
2	0.9330	0.9590	0.9920	0.9830
3	**0.9450**	0.9737	0.9920	**0.9881**
4	0.9405	0.9659	**0.9922**	0.9858
5	0.9434	**0.9765**	0.9905	0.9869
Average	0.9386	0.9680	0.9914	0.9857

Table 2. Performance measures vs. Measure Ratio *R*

Measure Ratio (*R*)	Jaccard Index*	Sensitivity*	Specificity*	Accuracy*
$R \geq 0.95$	0.6167	0.8833	0.9917	1.000
$R \geq 0.90$	0.9250	0.9667	1.000	1.000
$R \geq 0.85$	0.9625	0.9875	1.000	1.000
$R \geq 0.80$	0. 9917	1.0000	1.000	1.000
$R \geq 0.78$	1.0000	1.0000	1.000	1.000

*for the Measure Ratio R given in column one.

Table 3. Comparison of the proposed FCN with other algorithms.

Measure	Roychowdhury [4]	Marin et al [6]	Morales et al. [7]	Proposed
Jaccard Index	0.84	0.87	0.82	0.94
Sensitivity	0.92	0.92	0.93	0.97

5. CONCLUSIONS

In this paper, we propose an automatic method to segment the optic disc from fundus images for glaucoma to estimate the optic disc to cup ratio. The method employs a FCN called U-Net to label pixels that belong to optic area from ROI images. The FCN uses a color image with 224×224×3 as an input and a segmentation image with 224×224×1 as an output. Unlike other algorithms that need preprocessing and post processing, the proposed FCN segments the optic disc without any other pre/post processing. The results are promising. The FCN shows better performance than other existing algorithms in Jaccard index and sensitivity. In addition, processing time is less than 0.06 second per image. As future work, we plan to use deeper and more complex FCN architectures such as Mask R-CNN and GAN to improve segmentation accuracy and computation time.

ACKNOWLEDGMENT

This research was supported by the Intramural Research Program of the National Institutes of Health, National Library of Medicine, and Lister Hill National Center for Biomedical Communications. We thank Dr. Arturo Aquino from the University of Huelva, Spain for providing the MESSIDOR dataset. In addition, we acknowledge the help of the National Eye Institute staff in providing additional fundus images (AREDS dataset) to extend this work.

REFERENCES

[1] Glaucoma Research Foundation, https://www.glaucoma.org.
[2] Almazroa, A., Alodhayb, S., Raahemifar, K., and Lakshminarayanan, V., "Optic Cup Segmentation:Type-II Fuzzy Thresholding Approach and Blood Vessel Extraction", Clinical Ophthalmology, 11, 841-854 (2017).
[3] Kim J., Candemir, C. , Chew, E., and Thoma, G.R., "Region of Interest Detection in Fundus Images Using Deep Learning and Blood Vessel Information", The 31th IEEE Internation Symposium on Computer-Based Medical System, 357-362 (2018).
[4] Roychowdhury, S., Koozekanani, D. D., Kuchinka, S. N., and Parhi, K. K., "Optic Disc Boundary and Vessel Origin Segmentation of Fundus Images," IEEE Journal of Biomedical and Health Informatics, 20(6), 1562-1574 (2016).
[5] Foracchia, M., Grisan, E., and Ruggeri, A., "Detection of Optic Disc in Retinal Images by Means of a Geometrical Model of Vessel Structure," IEEE Transactions on Medical Imaging, 23(10), 1189-1195 (2004)
[6] Marin, D., Gegundez-Arias, M.E., Suero, A., and Bravo, J. M., "Obtaining optic disc center and pixel region by automatic thresholding methods on morphologically processed fundus images", Computer Methods and Programs in Biomedicine, 173-185 (2015).
[7] Morales, S., Naranjo, V., Angulo, J., and Alcaniz, M., "Atomatic Detection of Optic Disc Based on PCA and Mathematical Morphology", IEEE Transaction on Medical Imaging, 32(4), 369-376 (2013)
[8] Cheng, J., Liu, J., Xu, Y., Yin, F., Wong, D.W.K., Tan, N., Tao, D., Cheng, C., Aung, T., and Wong, T.Y., "Subpixel Classification Based on Optic Disc and Optic Cup Segmentation for Glaucoma Screening", IEEE Trans Med Imaging. 32(6), 1019-32 (2013).
[9] Yu, S., Xiao, D., and Kanagasingam, Y., "Machine Learning Based Automatic Neovascularization Detection on Optic Disc Region", Journal of Biomedical and Health Informatics, 22(3) (2018).
[10] Savelli, B., Bria, A., Galdran, A., Marrocco, C., and Molinara, M., "Illumination correction by dehazing for retinal vessel segmentation" IEEE 30th International Symposium on Computer-Based Medical Systems, 219-224 (2017).
[11] Son, , Park, S. J., and Jung, K., "Retina Vessel Segmentation in Fundoscopic Images with Generative Adversarial Networks", DLMIA (2017).
[12] Lim, C., Cheng, Y, Hsu, W., and Lee, M. L., "Integrated Optic Disc and Cup Segmentation with Deep Learning," IEEE 27th International Conference on Tools with Artificial Intelligence, 19(3), 162-169 (2015).
[13] Decencière, E., et al., "Feedback on a publicly distributed database: the Messidor database", Image Analysis & Stereology, 33(3), 231-234 (2014), http://messidor.crihan.fr/ download-en.php.
[14] Ronneberger, O., Fischer, P., Brox, T.,"U-Net: Convolutional Networks for Biomedical Image Segmentation", Medical Image Computing and Computer-Assisted Intervention (MICCAI), Springer, LNCS, 9351, 234--241 (2015).